Hindawi Publishing Corporation
Journal of Nanomaterials
Volume 2014, Article ID 108359, 8 pages
http://dx.doi.org/10.1155/2014/108359

Research Article

Fluorescein-Labeled Starch Maleate Nanoparticles as Sensitive Fluorescent Sensing Probes for Metal Ions

Suk Fun Chin,[1] Aressa Azman,[1] Suh Cem Pang,[1] and Sing Muk Ng[2]

[1] *Department of Chemistry, Faculty of Resource Science and Technology, Universiti Malaysia Sarawak, 94300 Kota Samarahan, Sarawak, Malaysia*
[2] *Faculty of Engineering, Computing and Science, Swinburne University of Technology, 93350 Kuching, Sarawak, Malaysia*

Correspondence should be addressed to Suk Fun Chin; sukfunchin@gmail.com

Received 4 July 2013; Revised 7 December 2013; Accepted 7 December 2013; Published 28 January 2014

Academic Editor: Alan K. T. Lau

Fluorescein 5(6)-isothiocyanate starch maleate (FISM) nanoparticles were prepared by covalently attached fluorescein 5(6)-isothiocyanate (FITC) with starch maleate. FISM nanoparticles with a mean particle size of 87 nm were formed via self-assembly upon precipitation in ethanolic solution. FISM nanoparticles were strongly fluorescent with maximum emission wavelength of 518 nm. The fluorescence of FISM nanoparticles can be quenched by silver (Ag^+) and lead (Pb^{2+}) ions in a concentration dependent manner. We have demonstrated the first use of FISM nanoparticles as cheap and effective fluorescent sensing probes for Ag^+ and Pb^{2+} ions with detection limits as low as 2.55×10^{-5} M and 3.64×10^{-5} M, respectively.

1. Introduction

Polysaccharides such as starch, chitosan, alginate, and dextran have received great interest as precursor materials for the preparation of nanoparticles as they are abundantly available, of low cost, renewable, and nontoxic in nature [1, 2]. Besides, these biopolymers are suitable to be used for various biomedical applications due to their unique properties that are biocompatible and biodegradable [3]. Recently, the use of polysaccharides as precursor materials for preparation of fluorescent nanoparticles has considerably increased [4–8]. Various polysaccharides-based fluorescent nanoparticles have been reported such as fluorescein-labeled starch acetates [9], fluorescein-labeled dextran propionate [10, 11], fluorescein-labeled dextrin nanoparticles [6], magnetic fluorescent alginate nanoparticles [12], and fluorescent chitosan nanoparticles [13–15] in pieces of literature. These fluorescent polysaccharides-based nanoparticles have been utilized in various applications such as bioimaging [16], biosensing, chemical sensing [17], pH sensing [18], and drug delivery [19].

Physical entrapment of fluorophores is one of the commonly used approaches to incorporate fluorescent molecules into nanoparticles due to its simplicity [7]. However, this type of physical entrapment approach suffers from several major setbacks such as possible leaching of fluorophores that subsequently leads to toxicity of the cell, contamination of biological samples, and incorrect signal measurements [20]. In order to overcome these problems, some researchers have attempted to covalently attach fluorophores onto polysaccharides molecules [9, 11]. Covalent attachment is proven to reduce the leaching of fluorophores, provide good photostability, enhance lifetime, and produce stable fluorescent signals [20].

Fluorescence quenching has been employed extensively for the detection and quantification of various metal ions due to its high sensitivity, ease of handling, low cost, portability, and the fact that it can deliver rapid results [21, 22]. Fluorescence quenching involves the use of highly fluorescent fluorophore where intensity would be greatly reduced or quenched completely in the presence of a target analyte. Many metal ions are known to be fluorescence quenchers that could be detected using this method [23].

In this work, we have successfully synthesized fluorescein 5(6)-isothiocyanate-labeled starch maleate (FISM) nanoparticles by covalently attaching fluorescein 5(6)-isothiocyanate (FITC) with starch maleate. The potential application of FISM

nanoparticles as sensitive fluorescent probes for heavy metal ions detection was demonstrated. Our results showed that FISM nanoparticles could act as sensing probes for selective detection of Ag^+ and Pb^{2+} ions in aqueous systems.

2. Materials and Methods

2.1. Materials. Native sago starch (*Metroxylon sagu*) powder was purchased from local market at Kuching (Sarawak, Malaysia). Fluorescein 5(6)-isothiocyanate (FITC) was obtained from Sigma (USA); dibutyltin dilaurate (DBTDL), maleic anhydride, 2-(dimethyl-amino) pyridine (DMAP), dimethyl sulfoxide (DMSO), sodium hydroxide, and sodium dihydrogen phosphate monohydrate were purchased from Merck (Hohenbrunn, Germany). N,N-Dimethylformamide (DMF) was purchased from J.T. Baker (Phillipsburg, USA) and absolute ethanol, disodium hydrogen phosphate, and acetic acid were purchased from HmbG Chemicals (Hamburg, Germany). Sodium acetate hydrated and sodium hydrogen carbonate were obtained from Bendosen Laboratory Chemicals (Bendosen, Norway). $AgNO_3$, $Ca(NO_3)_2$, $CO(NO_3)_2$, $Cr(NO_3)_2$, $Cu(NO_3)_2$, $HgCl_2$, $Mg(NO_3)_2$, $Ni(NO_3)_2$, $Pb(NO_3)_2$, $Zn(NO_3)_2$, and $Al(NO_3)_3$ were purchased from R&M Marketing (Essex, UK). Ultrapure water (18.2 MΩ·cm) obtained from a Water Purifying System (Model: ELGA, Ultra Genetic) was used throughout the experiments. Native sago starch powder and all chemicals were used without further purification.

2.2. Preparation of Fluorescein-Labeled Starch Maleate (FISM) Nanoparticles. Starch maleate was synthesized based on method adapted from Tay et al. [24, 25] and Li et al. [9] with slight modification. About 2.0 g of native sago starch powder (12.34×10^{-3} mole anhydroglucose unit) was dissolved in 50 mL of N,N-dimethylformamide (DMF). The solution was stirred for about 15–20 min at 90°C. Then 3.63 g of maleic anhydride (37.04×10^{-3} mole) and 30 μL DMAP were added into the mixture. The mixture was stirred continuously (900 rpm) at 90–95°C for 4 h. Subsequently, the mixture was cooled to room temperature and precipitated with ultra-pure water. The precipitate was rinsed several times with ultra-pure water to remove any unreacted salts.

For synthesis of FISM, 1.5 g of starch maleate reacted with various concentrations of FITC (0.05, 0.25, 0.5, 1.0, 2.0, and 3.0 mg/mL) in 10 mL DMSO for 6 h at 90–95°C. Also, 1.6 mL of DBTDL was added to the solution as a catalyst. The resulting FISM solution was added dropwise into ethanol to produce FISM nanoparticles via precipitation. The FISM nanoparticles were purified by dialyzing the samples using dialysis membranes against ultra-pure water for 24 h before being used for further study.

2.3. Characterization of FISM Nanoparticles

2.3.1. Spectroscopy Characterizations. The absorbance of FISM nanoparticles was recorded using a UV/Vis spectrophotometer (Model: JASCO V-630). Infrared spectra of the samples were characterized using a Fourier transformed infrared (FTIR) spectroscopy (Model: PerkinElmer). Sample was mixed into KBr/sample pellets and the FITR spectra were recorded within the wavenumber range of 4000–400 cm^{-1}. The fluorescence intensity was measured at room temperature using spectrofluorometer (Model: Cary Eclipse, Varian) at a fixed excitation wavelength of 495 nm. 100 μL of stock solution of FISM (2 mg/mL) in ultra-pure water was mixed with 2 mL of buffer solution in a cuvette. The fluorescence intensity of sample in buffer solution at different pH (4.0–12.0) was recorded at fixed emission wavelength of 518 nm. The excitation and emission slits were both set at 5.0 nm. The particle sizes and morphology of FISM nanoparticles were observed by using a transmission electron microscope (TEM) (Model: JEOL JEM-1230). The diameters of around 100 nanoparticles were measured randomly using the Smile-View software. Fluorescence image of FISM nanoparticles was obtained with inverted microscope system (Olympus, Model: IX51) with a 100W high pressure mercury lamp (Olympus, Model: BH2-RFL-T3) and digital color camera DCC (Olympus, Model: XC30).

2.3.2. Determination of Degree of Substitution (DS). DS of starch maleate was determined based on the method reported by Stojanovic et al. [26] with slight modifications. About 0.5 g of the starch maleate sample was added to 20 mL of 0.2 M NaOH solution. The mixture was stirred until the entire precursor was dissolved completely. The solution was transferred to a 100 mL volumetric flask, which was then filled up to the mark with ultra-pure water. 25 mL of the solution was transferred to Erlenmeyer flask, excess of NaOH solution in the sample was back titrated with 0.05 M of HCl using phenolphthalein as an indicator. Native starch sample was also titrated as the blank sample. The difference between the starch maleate sample and blank sample which were titrated in excess of NaOH was a measure of maleate content in the sample. The titration was repeated three times and the average volume of HCl was used for the calculations. The amount of carboxylic terminal (COOH) was determined using (1) and DS was calculated according to (2):

$$n\text{COOH} = (V_b - V) \cdot C_{\text{HCl}} \cdot 4, \tag{1}$$

$$\text{DS} = \frac{162 \times n\text{COOH}}{\text{Mds} - 99n\text{COOH}}, \tag{2}$$

where nCOOH is the amount of COOH (in mole) present in the sample; V_b is the volume of 0.05 M HCl (in mL) used for titration of blank; V is volume of HCl (in mL) used for the titration of starch maleate; C_{HCl} is the molarity of HCl solution and 4 is the ratio of the total volume of solution (100 mL); 162 g/mole is the molecular weight of anhydroglucose unit (AGU); Mds is the mass of dry sample (in g) and 99 g/mole is the net increase in the molecular weight of the maleate group substituted.

2.3.3. Labeling Efficiency (LE). The concentration of FITC grafted onto starch maleate was determined by correlating the fluorescence intensity of the sample to a calibration curve constructed from known concentration of free FITC

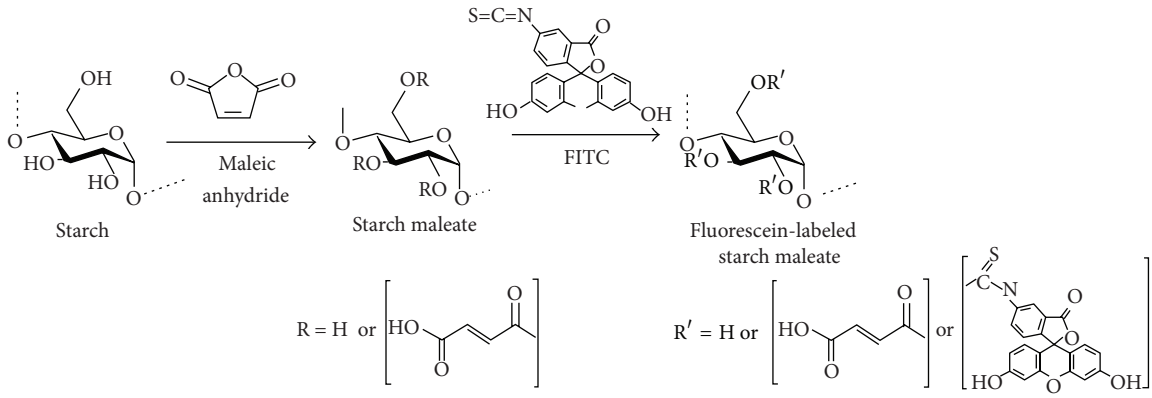

Figure 1: Schematic diagram of the reaction between starch, starch maleate, and fluorescein 5(6)-isothiocyanate starch maleate.

in DMSO. The degree of substitution (in percentage) of FITC in FISM sample was calculated according to

$$\%\text{FITC} = \frac{[\text{FITC}]}{[\text{FISM}]} \times 100, \quad (3)$$

where [FITC] is concentration of FITC in FISM sample (in mg/mL) and [FISM] is the concentration of FISM sample (in mg/mL).

3. Results and Discussion

3.1. Synthesis of FISM Nanoparticles. FISM nanoparticles were synthesized from native sago starch grafted with maleic and fluorophore groups. Starch was esterified using maleic anhydride and then labeled with FITC. DMF and DMSO were used as solvents instead of water during the synthesis of starch maleate (SM) and fluorescein-labeled starch maleate (FISM), as this esterification reaction would release water as a side product. As esterification reaction is a reversible reaction, this reaction can proceed in either the forward (left to right) or the reverse direction depending on conditions. Increasing the water content tends to drive the reaction in the reverse reaction, which is undesirable as the aim is to produce more of SM and FISM. Thus, DMF and DMSO were used as solvents to maintain the mixture with lower yield of water so that the equilibrium would give forward reaction to produce greater yield of product [27]. DMAP acted as a nucleophilic catalyst [28] for the esterification reaction with anhydrides, where it catalyzed the reaction of maleic anhydride and hydroxyl (OH) group of starch. DMAP attacked the anhydrides to form intermediate amide which was more reactive towards nucleophilic attack than the original anhydride. Starch molecules have OH groups that are able to act as nucleophiles, attacking the intermediate amide or the activated carbonyl carbon of maleic anhydride to produce starch maleate. For synthesis of FISM, DBTDL was used to catalyze the reaction between FITC molecules with starch maleate molecules by activating isothiocyanate molecules of FITC. The OH group of starch maleate attacked this activated isothiocyanate carbon atom which then further reacted by propagating the polymer to give thiocarbamate ester and regenerating the catalytic species [29].

The esterification processes through DMF/DMAP and DMSO/DBTDL systems represent an effective method for synthesizing fluorescent starch maleate. The labeling reaction was based on the covalent binding between the isothiocyanate group of FITC and the OH group of starch as illustrated by the scheme in Figure 1. The degree of substitution (DS) of starch maleate was determined to be 1.64, whereas DS of FITC onto starch maleate was 0.63%. The DS of starch maleate obtained from this study was higher as compared to the previously reported of 0.03–0.21 [25]. This could be due to the fact that the DMAP used in this study was a more effective catalyst as compared to NaOH used in the previous study.

3.2. Spectroscopy Characterizations. FTIR spectra of starch maleate (SM) and fluorescein 5(6)-isothiocyanate-labeled starch maleate (FISM) were shown in Figure 2. New absorption bands belonged to carbonyl group of maleate were observed in the spectra of starch maleate at 1728 and 1718 cm^{-1}. This observation suggested that the starch maleate was successfully formed during the esterification process. Besides, the absence of absorption peak that corresponded to ring anhydride carbonyl group at 1783 and 1857 cm^{-1} in starch maleate showed that the sample was not contaminated with maleic anhydride. The absorption peak at 1638 cm^{-1} was due to tightly bound water present in the samples, and this peak was also overlapped with the C=C stretching of maleate on the starch chain.

After the reaction of starch maleate with FITC, the intensity of absorption peaks at around 1638 cm^{-1} and 1653 cm^{-1} was observed to increase due to increase in C=C stretching present in FITC molecules and the formation of thiocarbamate bond of the fluorescein derivatives. This supported the suggestion that a reaction had taken place between isothiocyanate group in the fluorescein and the OH group of starch maleate.

The UV/Vis absorption spectra of FISM nanoparticles and free FITC in ultra-pure water (pH 6.8) and buffer solution of pH 9 were presented in Figure 3. FISM nanoparticles showed two broad absorption peaks at around 450 and

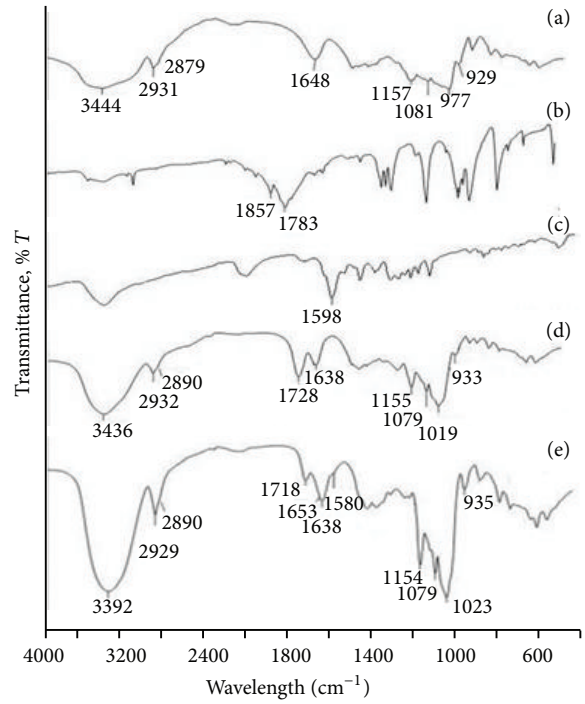

Figure 2: FTIR spectra of (a) native sago starch, (b) maleic anhydride, (c) FITC, (d) starch maleate, and (e) fluorescein 5(6)-isothiocyanate-labeled starch maleate (FISM) nanoparticles.

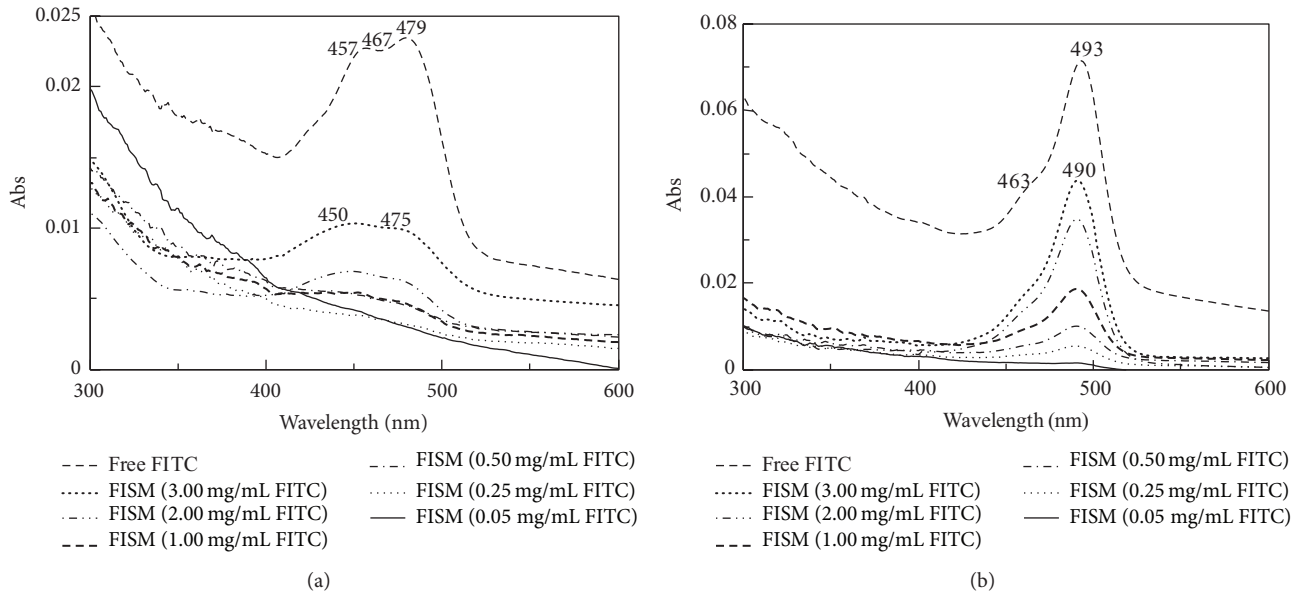

Figure 3: UV/Vis absorption of an aqueous suspension of free FITC and FISM nanoparticles with different concentrations of FITC in (a) ultra-pure water and (b) buffer solution of pH 9.

475 nm in water (pH ~ 6.8) which were close to the reported typical absorption peaks at 457, 467 and 479 nm for free FITC [30]. Both free FITC and FISM nanoparticles showed absorption maxima at around 490 nm in basic solution. These absorption peaks were not observed in the unlabeled starch maleate. The presence of the typical absorption peaks of FITC confirmed the presence of FITC in FISM.

The intensity of UV/Vis absorption of FISM was strongly dependent on the pH of the solution. The intensity of absorption was higher in basic solution as compared to acidic solution. This is because FITC is present in dianionic form and more soluble in basic condition [9, 28, 31]. However, FITC is mainly in monoanionic form [32] and has lower solubility in acidic solution.

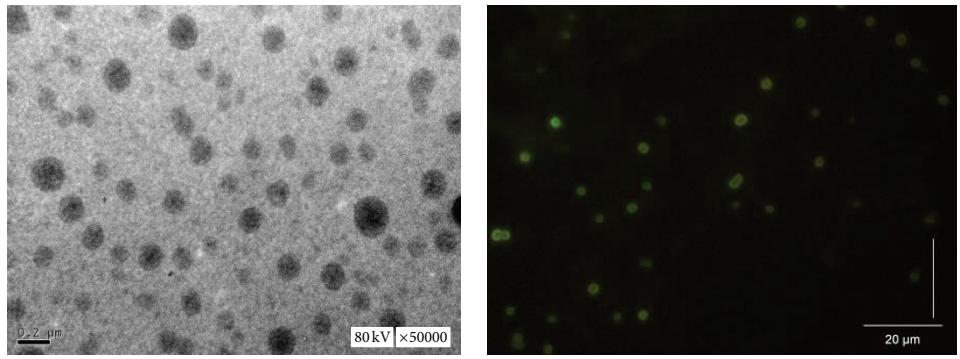

(a) (b)

Figure 4: (a) TEM micrograph and (b) fluorescence image of FISM nanoparticles.

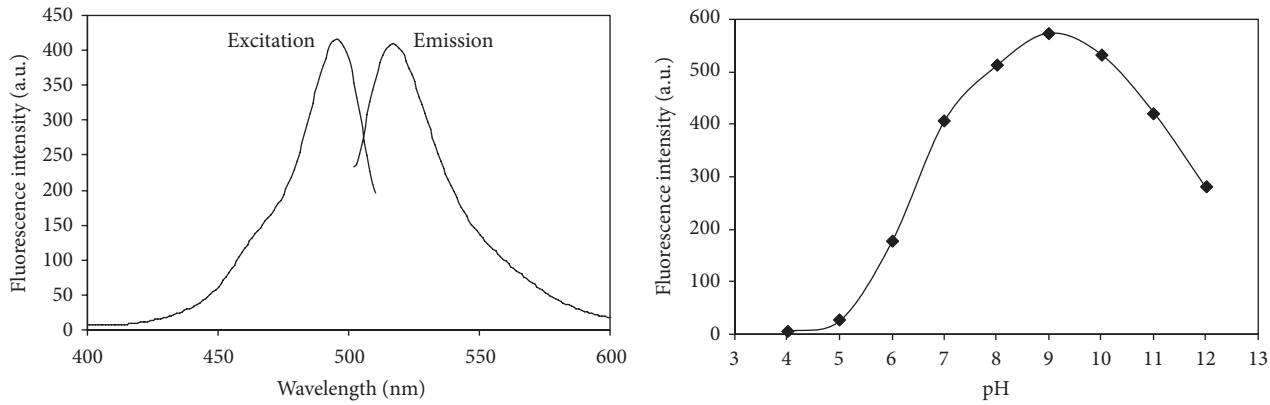

(a) (b)

Figure 5: (a) Excitation and emission spectra of FISM in buffered solution of pH 7 and (b) fluorescence intensity of FISM nanoparticles in various pH buffer solutions in the range 4 to 12. (λ_{ex} = 495 nm and λ_{em} = 518 nm).

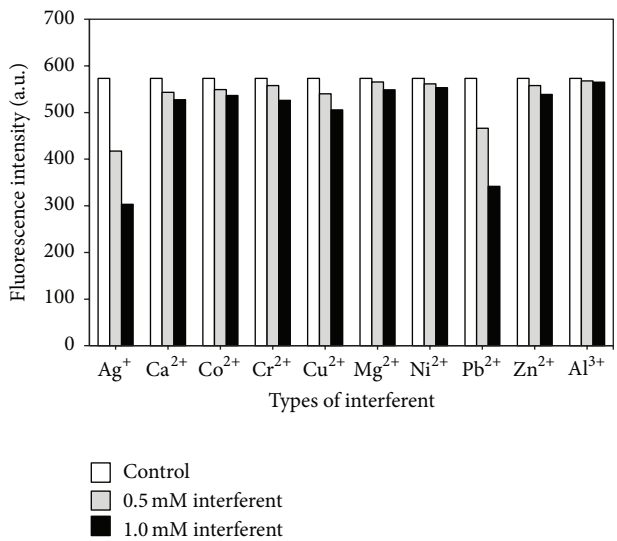

Figure 6: Effect of types of interferent on fluorescence intensity of FISM nanoparticles in pH 9 buffer solution.

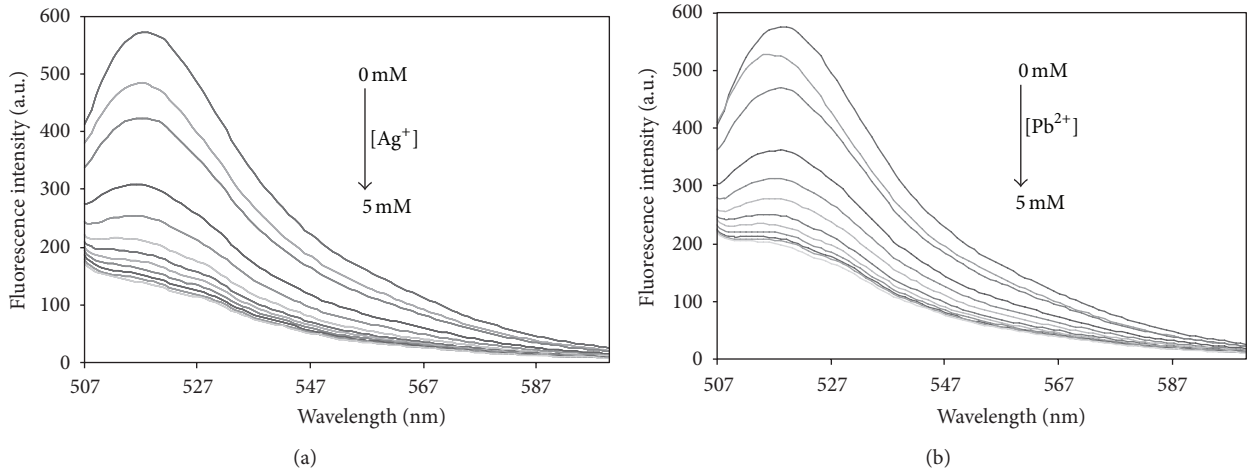

Figure 7: The fluorescence quenching curves of FISM by (a) Ag^+ and (b) Pb^{2+}, respectively.

3.3. Morphology of FISM Nanoparticles. FISM nanoparticles were observed to be discrete and spherical in shape as shown by the TEM in Figure 4. The maleated process imparted hydrophobicity and consequently prevented rapid aggregation and gelation of the starch-based nanoparticles in aqueous solution [24]. The mean particle size of the sample was around 87 nm. This further confirmed that starch maleate was self-assembled into nanospheres upon precipitation in ethanol.

3.4. Fluorescence Properties of FISM Nanoparticles. FISM nanoparticles showed an excitation and emission peak at 495 nm and 518 nm (Figure 5(a)). Effect of pH on the fluorescence intensity of FISM nanoparticles was shown in Figure 5(b). The FISM nanoparticles were pH sensitive due to carbonyl and hydroxyl groups of FITC attached onto starch maleate. The fluorescence intensity of FISM increased with increasing pH up to pH 9, and under this condition FITC was completely ionized and in its most fluorescent form. The observed high fluorescence intensity might be due to a more dianion species of FITC which was presented in a basic solution of FISM sample [9]. However, when pH was above 9, the fluorescence intensity of the FISM nanoparticles was observed to decrease. We speculated that FITC was unstable at extreme high pH and hydrolysis of the thiocarbamoyl linkage would occur and result in self-quenching. Therefore, pH 9 was chosen for all further experiments since the highest fluorescence intensity was obtained at this pH.

3.5. Analytical Characteristics. Figure 6 shows the corresponding fluorescence signal changes of FISM upon addition of 0.5 and 1.0 mM of various metal ions to the FISM suspension. The fluorescence intensity of FISM samples was observed to be quenched by most of the heavy metals ions tested in this study. As illustrated in Figure 7, more significant quenching was observed for Ag^+ and Pb^{2+} ions as compared to the other metal ions. This finding suggested direct interaction of the metal ions with the thiol group [33]

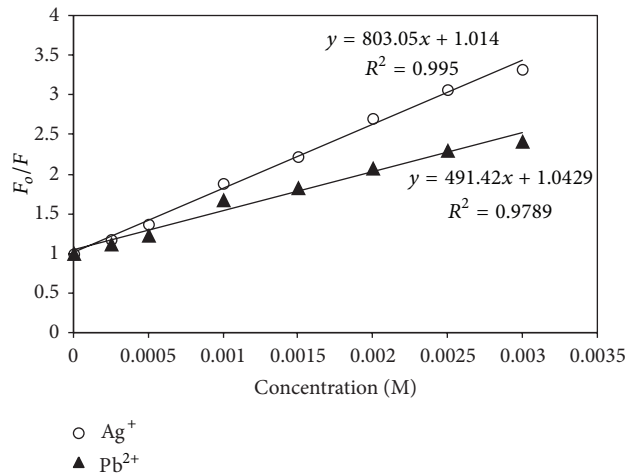

Figure 8: Stern-Volmer plots for fluorescence quenching of FISM nanoparticles by Ag^+ and Pb^{2+} in buffer solution of pH 9.

of FITC in FISM. Large amounts of Ag^+ and Pb^{2+} ions were bound to the FITC molecules which caused the fluorescence intensity of FISM to be significantly quenched.

Figure 7 depicts the fluorescence emission spectra changes upon addition of Ag^+ and Pb^{2+} to FISM nanoparticles in buffer solution of pH 9. The fluorescence intensity of FISM sample was quenched upon addition of Ag^+ and Pb^{2+} ions up to 5 mM, beyond which no more significant signal change was observed. The quenching data can be quantitatively presented in the Stern-Volmer plot (Figure 8), based on F_0/F versus $[Ag^+]$ and $[Pb^{2+}]$ according to [31]

$$\frac{F_0}{F} = 1 + K_{SV}[Q], \tag{4}$$

where F_0 and F are the fluorescence intensities at 518 nm in the absence and presence of varying amounts of Ag^+ and Pb^{2+}, respectively, K_{SV} and $[Q]$ are Stern-Volmer quenching

constant and concentration of the quenchers. Linear Stern-Volmer plots were observed for both Ag^+ and Pb^{2+} with slopes being equal to K_{SV}. Under optimum conditions, K_{SV} values for Ag^+ and Pb^{2+} ions were $8.3 \times 10^2\ M^{-1}$ and $5.4 \times 10^2\ M^{-1}$ and LOD values were determined to be 2.55×10^{-5} M and 3.64×10^{-5} M for Ag^+ and Pb^{2+} ions, respectively. This suggested that FISM could potentially be used for Ag^+ and Pb^{2+} ions detection with high sensitivity.

4. Conclusions

Novel FISM nanoparticles with a mean particle size of around 87 nm were successfully prepared via the precipitation method. These FISM nanoparticles exhibited high fluorescence intensity in buffer solution of pH 9. The results of this study demonstrated that these FISM nanoparticles could be used as cheap, effective fluorescent sensing probes for Ag^+ and Pb^{2+} ions with detection limits as low as 2.55×10^{-5} M and 3.64×10^{-5} M, respectively.

Conflict of Interests

The authors declare that they have no conflict of interests regarding the publication of this paper.

Acknowledgments

Financial support by the Ministry of Higher Education (MOHE) Fundamental Research Grant Scheme (FRGS), Grant no. 01(17)746/2010(32), and MyBrain (MyMaster) Program for graduate scholarship was gratefully acknowledged.

References

[1] D. R. Lu, C. M. Xiao, and S. J. Xu, "Starch-based completely biodegradable polymer materials," *Express Polymer Letters*, vol. 3, no. 6, pp. 366–375, 2009.

[2] O. Carp, D. Visinescu, G. Patrinoiu, A. Tirsoaga, C. Paraschiv, and M. Tudose, "Green synthetic strategies of oxide materials: polysaccharides-assisted synthesis. I. polysaccharides roles in metal oxides synthesis," *Revue Roumaine de Chimie*, vol. 55, no. 10, pp. 705–709, 2010.

[3] S. K. Nitta and K. Numata, "Biopolymer-based nanoparticles for drug, gene delivery and tissue engineering," *International Journal of Molecular Sciences*, vol. 14, pp. 1629–1654, 2013.

[4] S. N. A. Mohd Yazid, S. F. Chin, S. C. Pang, and S. M. Ng, "Detection of Sn(II) ions via quenching of the fluorescence of carbon nanodots," *Microchimica Acta*, vol. 180, pp. 137–143, 2013.

[5] S. F. Chin, S. N. A. Mohd Yazid, S. C. Pang, and S. M. Ng, "Facile synthesis of fluorescent carbon nanodots from starch nanoparticles," *Materials Letters*, vol. 85, pp. 50–52, 2012.

[6] C. Gonçalves, E. Torrado, T. Martins, P. Pereira, J. Pedrosa, and M. Gama, "Dextrin nanoparticles: studies on the interaction with murine macrophages and blood clearance," *Colloids and Surfaces B*, vol. 75, no. 2, pp. 483–489, 2010.

[7] X. Jia, X. Chen, Y. Xu, X. Han, and Z. Xu, "Tracing transport of chitosan nanoparticles and molecules in Caco-2 cells by fluorescent labeling," *Carbohydrate Polymers*, vol. 78, no. 2, pp. 323–329, 2009.

[8] K. Aslan, M. Wu, J. R. Lakowicz, and C. D. Geddes, "Fluorescent core-shell $Ag@SiO_2$ nanocomposites for metal-enhanced fluorescence and single nanoparticle sensing platforms," *Journal of the American Chemical Society*, vol. 129, no. 6, pp. 1524–1525, 2007.

[9] Y. Li, Y. Tan, Z. Ning, S. Sun, Y. Gao, and P. Wang, "Design and fabrication of fluorescein-labeled starch-based nanospheres," *Carbohydrate Polymers*, vol. 86, no. 1, pp. 291–295, 2011.

[10] H. Wondraczek, A. Kotiaho, P. Fardim, and T. Heinze, "Photoactive polysaccharides," *Carbohydrate Polymers*, vol. 83, no. 3, pp. 1048–1061, 2011.

[11] S. Hornig, C. Biskup, A. Gräfe et al., "Biocompatible fluorescent nanoparticles for pH-sensoring," *Soft Matter*, vol. 4, no. 6, pp. 1169–1172, 2008.

[12] J. Liu, Y. Zhang, T. Yang et al., "Synthesis, characterization, and application of composite alginate microspheres with magnetic and fluorescent functionalities," *Journal of Applied Polymer Science*, vol. 113, no. 6, pp. 4042–4051, 2009.

[13] P. Tallury, S. Kar, S. Bamrungsap, Y.-F. Huang, W. Tan, and S. Santra, "Ultra-small water-dispersible fluorescent chitosan nanoparticles: synthesis, characterization and specific targeting," *Chemical Communications*, no. 17, pp. 2347–2349, 2009.

[14] J. Zhao and J. Wu, "Preparation and characterization of the fluorescent chitosan nanoparticle probe," *Chinese Journal of Analytical Chemistry*, vol. 34, no. 11, pp. 1555–1559, 2006.

[15] A. M. de Campos, Y. Diebold, E. L. S. Carvalho, A. Sánchez, and M. J. Alonso, "Chitosan nanoparticles as new ocular drug delivery systems: in vitro stability, in vivo fate, and cellular toxicity," *Pharmaceutical Research*, vol. 21, no. 5, pp. 803–810, 2004.

[16] K. Park, "Polysaccharides-based near-infrared fluorescence nanoprobes for cancer diagnosis," *Quantitative Imaging in Medicine and Surgery*, vol. 2, no. 2, pp. 106–113, 2012.

[17] L. Basabe-Desmonts, D. N. Reinhoudt, and M. Crego-Calama, "Design of fluorescent materials for chemical sensing," *Chemical Society Reviews*, vol. 36, no. 6, pp. 993–1017, 2007.

[18] X. Zhang, *Study of novel nanoparticle sensors for food pH and water activity [Ph.D. thesis]*, Rutgers University, New Brunswick, NJ, USA, 2009.

[19] H. Katas and C. M. Wen, "Preparation and characterization of highly loaded fluorescent chitosan nanoparticles," *International Scholarly Research Network Pharmaceutics*, vol. 2011, Article ID 246162, 5 pages, 2011.

[20] A. Schulz, S. Hornig, T. Liebert, E. Birckner, T. Heinze, and G. J. Mohr, "Evaluation of fluorescent polysaccharide nanoparticles for pH-sensing," *Organic and Biomolecular Chemistry*, vol. 7, no. 9, pp. 1884–1889, 2009.

[21] B. Liu, Y. Bao, H. Wang et al., "An efficient conjugated polymer sensor based on the aggregation-induced fluorescence quenching mechanism for the specific detection of palladium and platinum ions," *Journal of Materials Chemistry*, vol. 22, no. 8, pp. 3555–3561, 2012.

[22] S. S. Tan, S. J. Kim, and E. T. Kool, "Differentiating between fluorescence-quenching metal ions with polyfluorophore sensors built on a DNA backbone," *Journal of the American Chemical Society*, vol. 133, no. 8, pp. 2664–2671, 2011.

[23] F.-Y. Wu, S. W. Bae, and J.-I. Hong, "A selective fluorescent sensor for Pb(II) in water," *Tetrahedron Letters*, vol. 47, no. 50, pp. 8851–8854, 2006.

[24] S. H. Tay, S. C. Pang, and S. F. Chin, "A facile approach for controlled synthesis of hydrophilic starch-based nanoparticles

from native sago starch," *Starch/Stärke*, vol. 64, pp. 984–990, 2012.

[25] S. H. Tay, S. C. Pang, and S. F. Chin, "Facile synthesis of starch-maleate monoesters from native sago starch," *Carbohydrate Polymers*, vol. 88, no. 4, pp. 1195–1200, 2012.

[26] Z. Stojanovic, K. Jeremic, S. Jovanovic, and M. D. Lechner, "A comparison of some methods for the determination on the degree of substitution of carboxylmethyl starch," *Starch/Starke*, vol. 57, pp. 79–83, 2005.

[27] S. C. Pang, S. F. Chin, S. H. Tay, and F. M. Tchong, "Starch-maleate-polyvinyl alcohol hydrogels with controllable swelling behaviors," *Carbohydrate Polymers*, vol. 84, no. 1, pp. 424–429, 2011.

[28] W. Li, L. Wu, D. Chen, C. Liu, and R. Sun, "DMAP-catalyzed phthalylation of cellulose with phthalic anhydride in [bmim]Cl," *BioResources*, vol. 6, no. 3, pp. 2375–2385, 2011.

[29] T. A. Smith, L. M. Bajada, and D. E. Dunstan, "Fluorescence polarization measurements of the local viscosity of hydroxypropyl guar in solution," *Macromolecules*, vol. 35, no. 7, pp. 2736–2742, 2002.

[30] B. Liu, S. Fletcher, M. Avadisian, P. T. Gunning, and C. C. Gradinaru, "A photostable, pH-invariant fluorescein derivative for single-molecule microscopy," *Journal of Fluorescence*, vol. 19, no. 5, pp. 915–920, 2009.

[31] H. Li, J. Zhai, and X. Sun, "Sensitive and selective detection of silver(I) ion in aqueous solution using carbon nanoparticles as a cheap, effective fluorescent sensing platform," *Langmuir*, vol. 27, no. 8, pp. 4305–4308, 2011.

[32] D. Zhang, K. Vangala, D. Jiang, S. Zou, and T. Pechan, "Drop coating deposition raman spectroscopy of fluorescein isothiocyanate labeled protein," *Applied Spectroscopy*, vol. 64, no. 10, pp. 1078–1085, 2010.

[33] E. M. Ali, Y. Zheng, H.-H. Yu, and J. Y. Ying, "Ultrasensitive Pb^{2+} detection by glutathione-capped quantum dots," *Analytical Chemistry*, vol. 79, no. 24, pp. 9452–9458, 2007.